Journal of
Applied Crystallography
ISSN 0021-8898
Editor: **Anke R. Pyzalla**

Facilitating protein crystal cryoprotection in thick-walled plastic capillaries by high-pressure cryocooling

Yi-Fan Chen, Mark W. Tate and Sol M. Gruner

J. Appl. Cryst. (2009). **42**, 525–530

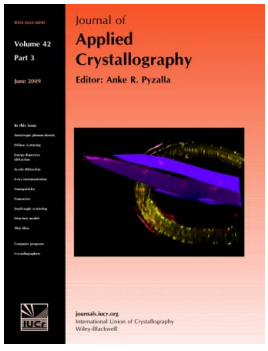

Journal of
Applied Crystallography
ISSN 0021-8898

Received 6 October 2008
Accepted 26 March 2009

Facilitating protein crystal cryoprotection in thick-walled plastic capillaries by high-pressure cryocooling

Yi-Fan Chen,[a,b] Mark W. Tate[c] and Sol M. Gruner[a,b]*

[a]Field of Biophysics, Cornell University, Ithaca, NY 14853, USA, [b]Cornell High Energy Synchrotron Source (CHESS), Ithaca, NY 14853, USA, and [c]Department of Physics, Cornell University, Ithaca, NY 14853, USA. Correspondence e-mail: smg26@cornell.edu

Many steps in the X-ray crystallographic solution of protein structures have been automated. However, the harvesting and cryocooling of crystals still rely primarily on manual handling, frequently with consequent mechanical damage. An attractive alternative is to grow crystals directly inside robust plastic capillaries that may be cryocooled and mounted on the beamline goniometer. In this case, it is still desirable to devise a way to cryoprotect the crystals, which is difficult owing to the poor thermal conductivity of thick plastic capillary walls and the large thermal mass of the capillary and internal mother liquor. A method is described to circumvent these difficulties. It is shown that high-pressure cryocooling substantially reduced the minimal concentrations of cryoprotectants required to cryocool water inside capillaries without formation of ice crystals. The minimal concentrations of PEG 200, PEG 400 and glycerol necessary for complete vitrification under pressure cryocooling were determined.

1. Introduction

Advances in structural genomics have spurred the development of automatic X-ray protein structure determination pipelines (for reviews, see Kuhn *et al.*, 2002; Pusey *et al.*, 2005; Berry *et al.*, 2006; Manjasetty *et al.*, 2008). These developments substantially reduce the costs of determining protein crystal structures and are resulting in a steady growth of novel structures deposited in the Protein Data Bank (Chandonia & Brenner, 2006; Levitt, 2007). Robot-assisted procedures are being developed for nearly every step in the X-ray protein crystallography pipeline, from gene cloning to X-ray data collection. One of the most challenging steps, harvesting and cryocooling crystals, still primarily relies on manual handling. A way to automate this step is to utilize robust plastic capillaries as crystal-growing containers (Potter *et al.*, 2004). Crystallization cocktails are dispensed into capillaries by, for example, robotic microfluidics-based techniques (Yadav *et al.*, 2005; Li *et al.*, 2006). The mother-liquor-filled capillary, with the crystals grown inside, may be subsequently placed in the X-ray beamline without the need to ever remove the crystal from its growth medium. However, cryoprotection of the protein crystals is difficult because the large thermal mass of the capillary and mother liquor and the heat transfer inefficiency of the plastic walls of the capillary greatly slow the cryocooling process, usually leading to the formation of ice crystals (Zheng *et al.*, 2005).

Cryocooling has been a routine practice in protein crystallography to mitigate radiation damage (for reviews, see Juers & Matthews, 2004*a*; Garman & Owen, 2006). A critical cooling rate must be achieved for vitrification and successful cryocooling. Reducing this threshold usually requires adding cryoprotectants. Generally, the higher the cryoprotectant concentration, the lower the critical cooling rate (Berejnov *et al.*, 2006). However, high cryoprotectant concentrations may not only cause damage to crystals and interfere with protein molecules, but also obstruct the crystallization screening process.

Previous reports from our laboratory have demonstrated a high-pressure method to cryocool protein crystals in cryoloops, frequently without the need for adding external cryoprotectants (Kim *et al.*, 2005). The formation of high-density amorphous (HDA) ice within high-pressure cryocooled crystals was observed and it was postulated that this accounts for the successful cryocooling in the absence of cryoprotectants (Kim *et al.*, 2008). Indeed, in the case of thaumatin, the high salt content of its mother liquor alone was all that was required to high-pressure cryocool crystals inside a thick-walled polycarbonate capillary, even though the cooling rate was markedly slower than with a cryoloop (Kim *et al.*, 2007). While this was true for thaumatin, it is not true for all mother liquors.

In the work reported here, we sought to investigate the minimal concentrations of common cryoprotectants sufficient to high-pressure vitrify aqueous solutions in thick-walled polycarbonate capillaries. The logic behind this study is simple. Added solutes tend to promote vitrification; therefore, if one determined a low concentration of a cryoprotectant

sufficient to pressure-cryocool water in capillaries, the additional salts of crystallization cocktails would result in solutions that were even easier to successfully pressure-cryocool. Then, simply by substituting the low-cryoprotectant solution for pure water when mixing cocktails for crystallization trials, one would be assured that any resulting crystal would have a very high probability of being successfully pressure-cryocooled in the capillary. Thus, the minimal cryoprotectant solutions would serve as nearly universal starting points for crystallization trials and successful high-pressure cryoprotection in capillaries.

Here, polyethylene glycol (PEG) 200, PEG 400 and glycerol were studied, owing to their prevalence in X-ray cryocrystallography (Garman & Owen, 2008). While these cryoprotectants at the minimally required concentrations are not guaranteed to be benign in all crystallization trials, they are

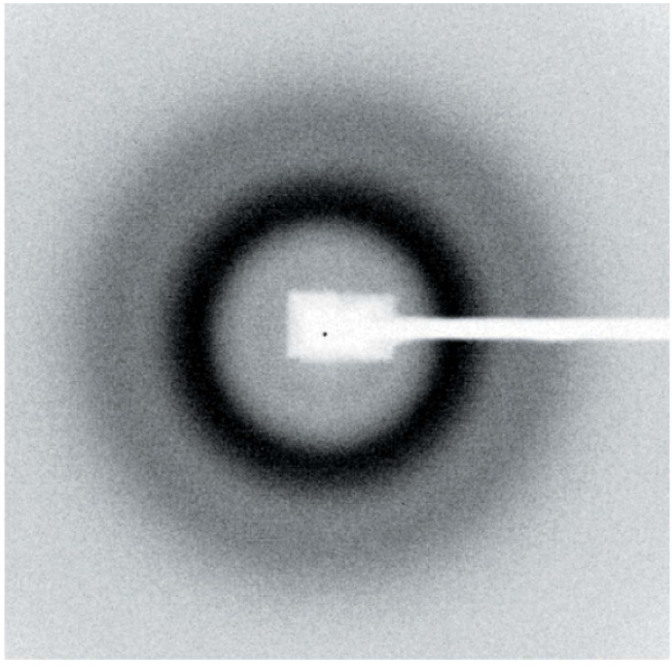

(*a*)

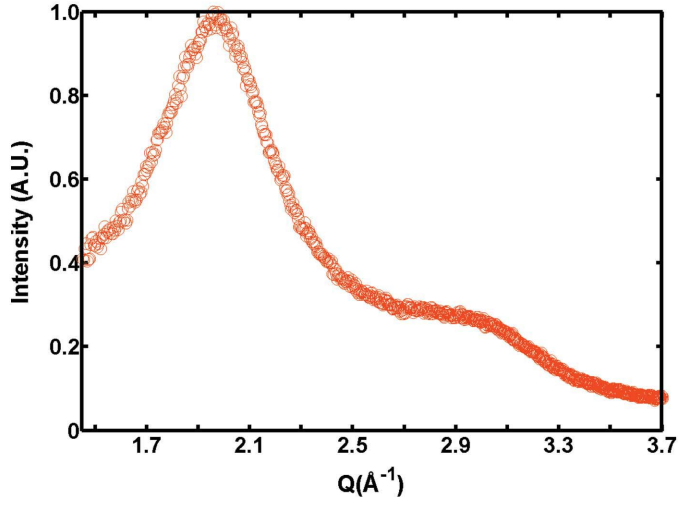

(*b*)

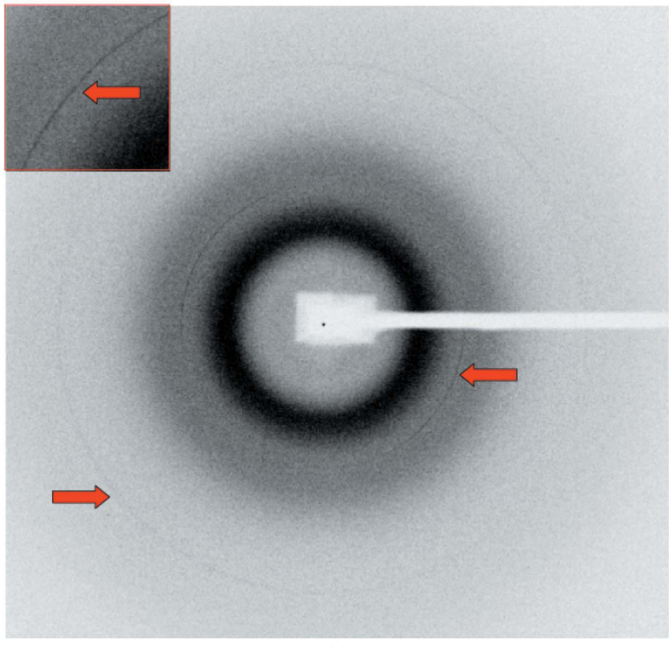

(*c*)

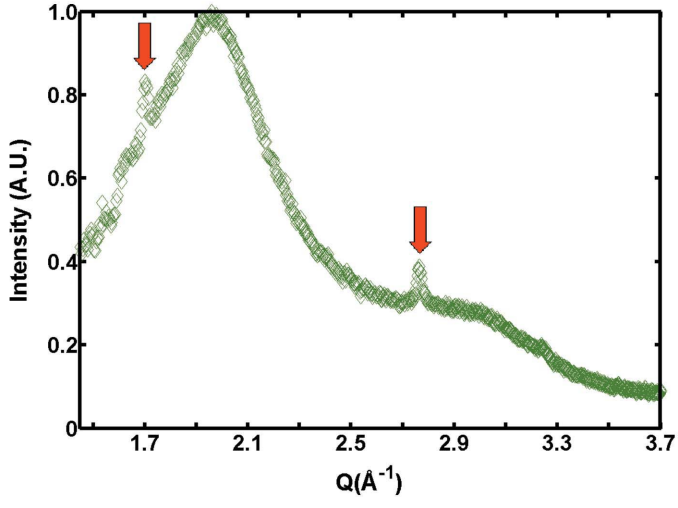

(*d*)

Figure 1
Diffraction images and diffraction intensity profiles of successful (*a*), (*b*) and unsuccessful (*c*), (*d*) cryocooling trials. Samples having a trace of crystalline ice features, indicated by the arrows in (*c*) and (*d*), are regarded as unsuccessful trials. The inset in (*c*) is shown at enhanced contrast to show more clearly a sharp but weak crystalline ice line. Note that the scattering features of polycarbonate walls of the capillaries (innermost diffuse ring) seen in (*a*) and (*c*) were subtracted (see text for detail) and not shown in (*b*) and (*d*). The primary broad peaks in (*b*) and (*d*) are from the amorphous water phase.

expected to be compatible with the vast majority. X-ray diffraction patterns of RNase A crystals grown in a comparable condition were also collected to demonstrate applicability to a real protein system.

2. Experimental

2.1. Sample preparation and data collection

PEG 200 (Alfa Aesar and Hampton Research), PEG 400 (Alfa Aesar) and glycerol (USB Corporation and Hampton Research) were used to prepare various cryoprotectant solutions without further purification. Prepared solutions were loaded by capillary action into polycarbonate capillaries (catalog No. 8-000-1000, Drummond Scientific) of inner diameter 300 µm, outer diameter 900 µm and length 15 mm. A small amount of highly viscous NVH oil (catalog No. HR3-611, Hampton Research) was used to seal the ends of the capillaries to prevent evaporation. The sample volume was ~0.8 µl. Samples were cryocooled with high-pressure cryocooling, as described by Kim *et al.* (2005). In short, samples were pressurized to 1800–2000 bar (180–200 MPa) with helium gas in a high-pressure vessel at room temperature and subsequently cooled at this pressure to liquid-nitrogen temperature, 77 K. Pressure was vented while samples remained at 77 K. The high-pressure cryocooled samples were stored at 77 K prior to X-ray diffraction experiments. Care was taken to ensure that all transfers and X-ray diffraction were performed at cryogenic temperatures.

Lyophilized bovine pancreatic RNase A powder (catalog No. R5125, Sigma–Aldrich) was used for crystallization without further purification. A modified hanging-drop method was employed for growing RNase A crystals in the aforementioned polycarbonate capillaries: the reservoir solution containing 0.1 *M* sodium acetate (pH 6.0), 30%(*v*/*v*) saturated ammonium sulfate, 50%(*v*/*v*) saturated sodium chloride and 10%(*v*/*v*) glycerol was mixed with the same volume of 24 mg ml^{-1} RNase A solution. The mixture was injected into a polycarbonate capillary and equilibrated against the reservoir solution inside a tape-sealed crystallization well by sticking the capillary to the tape. Crystals with a size of ~170 × 180 × 100 µm were observed in the capillaries after a week of incubation. Compared with the method described by Chatani *et al.* (2002), the presence of 10%(*v*/*v*) glycerol is the only difference in these crystallization conditions. This demonstrates that, in some cases, adding a small amount of cryoprotectant does not disturb the established crystallization conditions considerably. High-pressure cryocooling of the RNase A crystals followed the same procedure as described above.

X-ray diffraction data were collected at ambient pressure with Cu $K\alpha$ radiation from a Bruker Nonius FR 591 X-ray generator operated at 40 kV and 50 mA. Diffraction images were recorded with a Rigaku R-AXIS II image-plate detector. During data collection, samples were kept in a cold nitrogen stream (Oxford Cryosystem 700) at 80 or 85 K.

A background scattering image was also collected from the empty capillary in the following way: a rapid temperature increase, caused by temporarily blocking the nitrogen gas stream, emptied the capillary containing the cryoprotectant solution as a result of a sudden release of the helium gas dissolved in the solution. Hence, the only difference between data and background images was the presence or absence of the solution, reducing potential data misinterpretation from sources such as variation of capillaries. Each cryoprotectant solution sample thereby had a dedicated background diffraction image.

The diffuse rings seen in Fig. 1(*a*) arose from the polycarbonate walls of the capillary (innermost ring) and from the water (outermost ring). The plastic capillaries used in these experiments had 300 µm-thick polycarbonate walls and an inner diameter of 300 µm. Thus, the total path length of polycarbonate was 600 µm. The intensity of the polycarbonate scatter is a consequence of the wall thickness, coupled with long exposures in order to measure accurately the diffuse water ring (see §2.2). The intensity of the diffuse plastic scatter can be reduced by the use of capillaries with thinner walls. In our experience, however, even the diffuse plastic scatter does not impede protein diffraction analysis from most crystals that fill the capillary (§3.3; see also, *e.g.*, Kim *et al.*, 2007). No special crystallographic analysis programs were required.

2.2. Data analysis

Diffuse scattering from capillaries and other background sources was subtracted with the background images from the aforementioned method. The sample-to-detector distance was calibrated with the Bragg peaks of hexagonal ice (Blackman & Lisgarten, 1957) produced by heating the cryoprotectant solution samples to above 200 K. The azimuthally integrated diffraction profiles were fitted with Gaussian functions in the vicinity of the main diffuse peaks to obtain peak positions.

Since the boundary between successfully and unsuccessfully cryocooled samples can be ambiguous, a criterion was desired to discern the completeness of vitrification. Only samples showing no sharp Bragg diffraction of crystalline ice were regarded as being successfully cryocooled (Figs. 1*a* and 1*b*). Such samples displayed diffraction profiles featuring vitreous ice characteristics (Kim *et al.*, 2008). On the other hand, diffraction images showing a trace of sharp crystalline ice features caused the sample to be classified as unsuccessfully frozen even though vitreous ice may have been the dominant water phase in these samples (Figs. 1*c* and 1*d*).

3. Results and discussion

3.1. Success rate of vitrification

For screening protein crystallization conditions, hundreds or even thousands of trials are often set up to sample many conditions. In such a context, the fraction of trials that lead to successfully cryocooled crystals is more pertinent to high-throughput protein structure determination. Toward this end, the success rate was used to assess the ability of a cryopro-

Table 1
Comparison of the minimal concentrations required for vitrification using high-pressure cryocooling and flash cooling.

The concentrations for achieving ~70% success rate are listed for high-pressure cryocooling. Data for flash cooling were obtained from McFerrin & Snell (2002) and Berejnov *et al.* (2006). Note samples in the present study were prepared in capillaries, while the references adopted Hampton Research CryoLoops (McFerrin & Snell, 2002) or MiTeGen MicroMounts (Berejnov *et al.*, 2006).

Cryoprotectant†	High-pressure cryocooling	Flash cooling
PEG 200	15%(*v*/*v*)	35.7–37.5%(*v*/*v*)
PEG 400	10%(*v*/*v*)	>35%(*v*/*v*)
Glycerol	8%(*v*/*v*)	31.7–33.3%(*v*/*v*)

† Sample volumes are ~0.8 µl in this study and 0.5–1.0 µl in that of Berejnov *et al.* (2006), whereas sample volumes were not specified by McFerrin & Snell (2002).

tectant to vitrify water under our conditions. A statistically meaningful number of samples were prepared at each concentration to measure the success rate for a variety of cryoprotectant conditions. 'Pure' cryoprotectant solutions (*i.e.* with no added salts) are generally more difficult to vitrify than ordinary crystallization cocktails containing the same amount of cryoprotectant. Hence, higher success rates than shown here are expected when high-pressure cryocooling is applied to crystallization cocktails.

Fig. 2 shows the success rate of vitrification as a function of concentration for the three high-pressure cryocooled cryoprotectant solutions. PEG 400 and glycerol provide more reliable performance than PEG 200. Both reach a success rate of nearly 100% at the concentration of 15%(*v*/*v*), whereas 15% PEG 200 shows a relatively lower success rate of ~80%. None of the investigated cryoprotectant solutions successfully vitrified water at concentrations below 5%. A 70% success rate can be achieved by 10% PEG 400 and 8% glycerol solutions. These concentrations are much lower than the minimal concentrations required for vitrifying water at ambient pressure (McFerrin & Snell, 2002; Berejnov *et al.*, 2006). A comparison of the minimal concentrations for a 70% success rate with different cryocooling techniques is summarized in Table 1. Note that the minimal concentrations for flash cooling were obtained from cryomount-held samples designed for fast cooling. Even higher concentrations are needed for flash cooling the more slowly cooled polycarbonate capillaries. This demonstrates the efficacy of high-pressure cryocooling in facilitating vitrification.

3.2. Diffuse peak position and concentration

It was also observed that the positions of the diffuse peaks scattered by cryoprotectant solutions correlated with the specific cryoprotectants and concentrations (Fig. 3). The concentration dependence of the diffuse peak position rises steeply at first and then more slowly at higher concentrations. The diffuse peak positions largely reflect the intermolecular distances between the O atoms of water molecules. A similar trend was also seen in Fig. 4 of Juers & Matthews (2004*b*). It is emphasized that the diffuse peak position cannot be a direct indicator of density when comparing solutions with different compositions. For example, glycerol solutions of various concentrations, when vitrified at ambient pressure, have nearly identical diffuse peak positions, even though their densities vary.

Nevertheless, the diffuse peak position is capable of being a density indicator for a given solution when it is subjected to physical perturbations. In other words, a displacement of the diffuse peak corresponds to the change in density of a fixed constituted solution. Were the density of such a solution given, the density modified by pressure or temperature perturbations could be derived from the relative positions of the shifted and the initial peaks. The density of a given high-pressure cryocooled cryoprotectant solution can thereby be inferred from its flash-cooled counterpart *via*

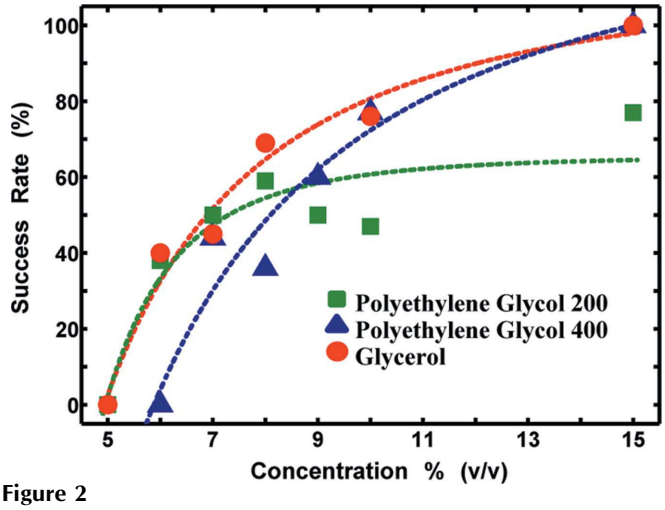

Figure 2
Success rate of vitrification *versus* concentration for high-pressure cryocooled PEG 200, PEG 400 and glycerol solutions. A ~70% success rate is achieved by 8%(*v*/*v*) glycerol and 10%(*v*/*v*) PEG 400. The curves are low-order polynomial fits simply to guide the eye.

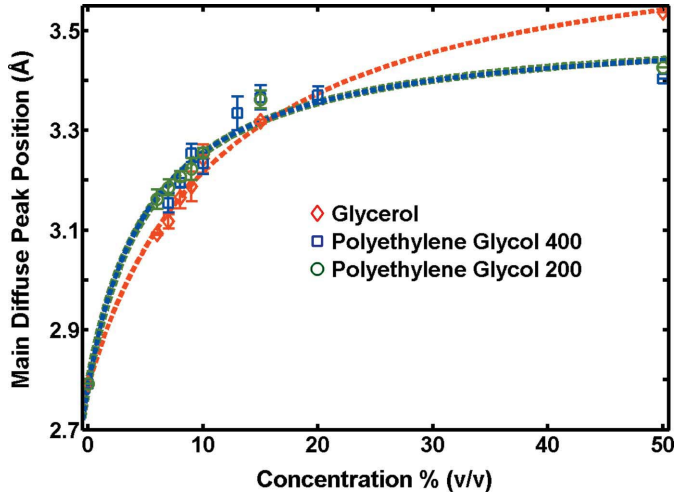

Figure 3
Diffuse peak position of vitreous ice as a function of concentration. The curves are low-order polynomial fits simply to guide the eye, and the data point for pure water (*i.e.* 0%*v*/*v*) was obtained from Tulk *et al.* (2002).

Table 2
Summary of crystallographic statistics for a high-pressure cryocooled RNase A crystal grown in the presence of 10%(*v*/*v*) glycerol inside a polycarbonate capillary.

Values for the high-resolution shell are shown in parentheses.

Space group	$P3_221$
Cell dimensions	
a, *b*, *c* (Å)	64.0, 64.0, 63.2
α, β, γ (°)	90, 90, 120
Mosaicity (°)	0.4†
Resolution range (Å)	27.7–2.0 (2.1–2.0)
$R_{\rm merge}$	0.062 (0.126)
Total observations	2150 (315)
Unique observations	2023 (283)
$I/\sigma(I)$	8.6 (4.1)
Completeness (%)	19.9 (20.0)

† The mosaicity was estimated by standard programs without deconvoluting the beam-smearing effect intrinsic to the rotating anode X-ray generator. The actual mosaicity of the sample itself will be smaller.

$$\rho' = \rho d/d', \tag{1}$$

where ρ' and d' are, respectively, the density and peak position of a high-pressure cryocooled solution while ρ and d are those of a flash-cooled solution.

Information with respect to the density of a cryoprotectant solution is of tremendous importance to cryopreservation of protein crystals. Juers & Matthews (2001) argued that the differential volume changes arising from protein molecules, crystals and mother liquors upon cooling, at least in part, accounted for damage imposed by cryocooling. Choosing a cryoprotectant condition that compensates for the differential volume changes would significantly diminish cryocooling-related damage.

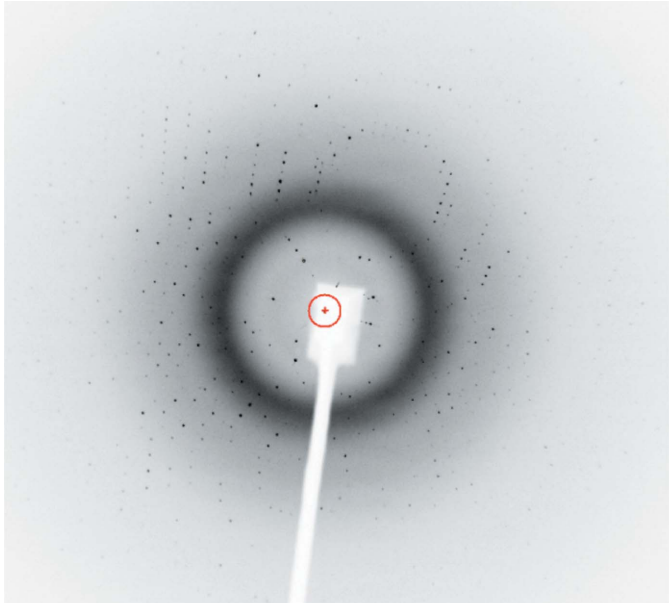

Figure 4
X-ray diffraction pattern of a high-pressure cryocooled RNase A crystal grown in the presence of 10%(*v*/*v*) glycerol inside a polycarbonate capillary. The crystal diffracted beyond 2 Å and the mosaicity is 0.4°. Note the absence of sharp crystalline ice lines, which indicates successful cryocooling.

3.3. Protein diffraction

Fig. 4 shows a representative protein diffraction pattern obtained with a high-pressure cryocooled RNase A crystal, grown in a 10%(*v*/*v*) glycerol-containing mother liquor inside a polycarbonate capillary. No attempt was made to acquire a complete data set. Statistics for several frames of this sample are shown in Table 2. In our experience, the mosaicity improves with a faster cooling rate, although the cooling rate is limited by the thermal mass of the thick-walled plastic capillaries that were used. Thinner-walled capillaries (*e.g.* X-ray glass capillaries) would increase the cooling rate and decrease the diffuse plastic scatter. Even so, analysis of diffraction from crystals cryocooled in these capillaries is straightforwardly performed [see the example given by Kim *et al.* (2008)].

4. Conclusions

In this study, we showed that high-pressure cryocooling substantially reduced the cryoprotectant concentrations required to vitrify polycarbonate capillary contents. In most cases, 8% glycerol, 10% PEG 400 and 15% PEG 200 were sufficient to cryocool otherwise pure water in capillaries. Even lower minimal concentrations are expected for crystallization cocktails. These results are impressive when compared with ∼33.3% glycerol, >35% PEG 400 and ∼37.5% PEG 200 needed for flash cooling crystals in Hampton Research CryoLoops or MiTeGen MicroMounts. Data collected from an RNase A crystal show that the minimum cryoprotectant concentrations determined by bulk solution vitrification can be extended to a real crystal system, and neither the glycerol, plastic capillary scatter or pressure impeded the data collection or data processing.

The low minimal concentrations of glycerol, PEG 400 and PEG 200 are expected to be compatible with many crystallization cocktails during crystallization trials, thereby facilitating automation of the crystal growing and cryocooling steps in the crystallization pipeline. Obviously, this requires an automated high-pressure cryocooling apparatus. We are confident that such an apparatus may be built by straightforward engineering of the existing apparatus.

The diffuse peak position, reflecting the O···O intermolecular distances of water molecules and related to the density of a cryoprotectant solution, was observed to depend on concentration. This relation may provide a guideline for selecting an optimal cryoprotectant condition in which the mismatch in volume changes of protein molecules, crystals and mother liquors upon cooling are minimized.

The authors would like to thank Drs Edward Snell, George DeTitta and other scientists at the Hauptman–Woodward Institute for their advice; and Gil Toombes, Lucas Koerner, Buz Barstow and Nozomi Ando for discussion and encouragement. This work was supported by NIH-NIGMS Protein Structure Initiative II *via* award U54-GM074899 and DOE grant DE-FG02-97ER62443. CHESS is supported by NSF and NIH *via* NSF award DMR-0225180.

References

Berejnov, V., Husseini, N. S., Alsaied, O. A. & Thorne, R. E. (2006). *J. Appl. Cryst.* **39**, 244–251.

Berry, I. M., Dym, O., Esnouf, R. M., Harlos, K., Meged, R., Perrakis, A., Sussman, J. L., Walter, T. S., Wilson, J. & Messerschmidt, A. (2006). *Acta Cryst.* D**62**, 1137–1149.

Blackman, M. & Lisgarten, N. D. (1957). *Proc. R. Soc. London Ser. A*, **239**, 93–107.

Chandonia, J. & Brenner, S. E. (2006). *Science*, **311**, 347–351.

Chatani, E., Hayashi, R., Moriyama, H. & Ueki, T. (2002). *Protein Sci.* **11**, 72–81.

Garman, E. F. & Owen, R. L. (2006). *Acta Cryst.* D**62**, 32–47.

Garman, E. F. & Owen, R. L. (2008). *Methods Mol. Biol.* **364**, 1–18.

Juers, D. H. & Matthews, B. W. (2001). *J. Mol. Biol.* **311**, 851–862.

Juers, D. H. & Matthews, B. W. (2004*a*). *Q. Rev. Biophys.* **37**, 105–119.

Juers, D. H. & Matthews, B. W. (2004*b*). *Acta Cryst.* D**60**, 412–421.

Kim, C. U., Chen, Y.-F., Tate, M. W. & Gruner, S. M. (2008). *J. Appl. Cryst.* **41**, 1–7.

Kim, C. U., Hao, Q. & Gruner, S. M. (2007). *Acta Cryst.* D**63**, 653–659.

Kim, C. U., Kapfer, R. & Gruner, S. M. (2005). *Acta Cryst.* D**61**, 881–890.

Kuhn, P., Wilson, K., Patch, M. G. & Stevens, R. C. (2002). *Curr. Opin. Chem. Biol.* **6**, 704–710.

Levitt, M. (2007). *Proc. Natl Acad. Sci. USA*, **104**, 3183–3188.

Li, L., Mustafi, D., Fu, Q., Tereshko, V., Chen, D. L., Tice, J. D. & Ismagilov, R. F. (2006). *Proc. Natl Acad. Sci. USA*, **103**, 19243–19248.

Manjasetty, B. A., Turnbull, A. P., Panjikar, S., Bussow, K. & Chance, M. R. (2008). *Proteomics*, **8**, 612–625.

McFerrin, M. B. & Snell, E. H. (2002). *J. Appl. Cryst.* **35**, 538–545.

Potter, R. R., Hong, Y. S. & Ciszak, E. M. (2004). *J. Appl. Cryst.* **37**, 500–501.

Pusey, M. L., Liu, Z.-J., Tempel, W., Praissman, J., Lin, D., Wang, B.-C., Gavira, J. A. & Ng, J. D. (2005). *Prog. Biophys. Mol. Biol.* **88**, 359–386.

Tulk, C. A., Benmore, C. J., Urquidi, J., Klug, D. D., Neuefeind, J., Tomberli, B. & Egelstaff, P. A. (2002). *Science*, **297**, 1320–1323.

Yadav, M. K., Gerdts, C. J., Sanishvili, R., Smith, W. W., Roach, L. S., Ismagilov, R. F., Kuhn, P. & Stevens, R. C. (2005). *J. Appl. Cryst.* **38**, 900–905.

Zheng, B., Gerdts, C. J. & Ismagilov, R. F. (2005). *Curr. Opin. Struct. Biol.* **15**, 548–555.